Table 1. Comparison of Re, Cr and U enrichment levels in modern anoxic marine sediments

Element	Upper Crust Concentration[1]	Average Conc.[1] In Modern[2] Anoxic Marine Sediments	Enrichment Factor[3]
Re	0.2–0.4	65.5	65.5
Cr	85	94.6	1.1
U	2.8	11.1	4.0

[1] Re in ppb; Cr and U in ppm

[2] Modern data defined as datasets with an age younger than 1 Ma

[3] Enrichment factor = anoxic sediment conc. / upper crust conc.

Re data: Esser and Turekian (1993); Peucker-Ehrenbrink and Jahn (2001); Dubin and Peucker-Ehrenbrink (2015); this study

Cr data: McLennan (2001); Reinhard et al. (2013a)

U data: McLennan (2001); Partin et al. (2013)

Table 2. Re burial rates in modern marine sediments. Basin mass accumulation rates are listed for anoxic sediments only. Oxygen penetration depth is given for suboxic and oxic sediments where available. Italicized names under the "Sampled Sediments" column are sub-basins within the same margin (in bold) and from which an arithmetic average is taken to represent the overall margin burial rate. Only center-justified values under the "Re Burial Rate" column are used in calculating weighted averages. This is done for the suboxic and oxic sinks; the modern anoxic sink burial rate is calculated from Cariaco Basin data (Supplementary information).

Sampled Sediments	Redox State	O_2 Penetration Depth (cm)	Basin MAR ($g\ cm^{-2}yr^{-1}$)	Re Burial Rate ($ng\ cm^{-2}yr^{-1}$)	Areal Extent (cm^2)	Weighing Factor	Representative Sink Re Burial Rate, b_i ($ng\ cm^{-2}yr^{-1}$)	References
OXIC								
Pelagic Sediments	oxic			1.2×10^{-5} [a]	2.7×10^{18} [b]	78.4%	1.6×10^{-3}	Colodner (1991)
Oxic Continetal Margins				7.4×10^{-3}	7.4×10^{17} [c]	21.6%		
Sea of Japan	oxic to suboxic			1.1×10^{-4}				Crusius et al. (1996); Dalai et al. (2005)
Lomonosov Ridge	oxic			4.3×10^{-4} [d]				Poirier & Hillaire-Marcel (2011)
NW US Margin, St 6, 8	oxic	1.5-5		1.4×10^{-3}				Morford et al. (2005)
African Margin, 2BC, 3BC	oxic	>3		2.8×10^{-2}				Morford and Emerson (1999); Morford et al. (2005)
SUBOXIC							0.41	
African Margin, 1BC	suboxic	0.9		0.42	8.0×10^{14} [e]	4.1%		Morford and Emerson (1999); Morford et al. (2005)
Laurentian Trough	suboxic	0.4-0.8		0.33	2.4×10^{15} [f]	12.4%		Sundby et al. (2004)
Buzzards Bay	suboxic	0.25-0.85		0.56	6.2×10^{12} [g]	0.03%		Morford et al. (2009)
Hingham Bay	suboxic	0.2-0.6		1.04	3.4×10^{11} [h]	0.002%		Morford et al. (2009)
Gulf of California				1.45	8.0×10^{14}	4.1%		Colodner et al. (1993)
Carmen	suboxic			1.4				Colodner et al. (1993)
San Pedro Matir	suboxic			1.5				Colodner et al. (1993)
Californian Borderlands				0.855	8.0×10^{14}	4.1%		Colodner et al. (1993)
Santa Barbara	suboxic	0-0.5 [i]		0.7				Colodner et al. (1993)
San Clemente	suboxic	0.4		0.55				Morford et al. (2005)
San Nicolas	suboxic	0.1		1.4				Morford et al. (2005)
Santa Cruz	suboxic	0.1		0.77				Morford et al. (2005)
W. American Margin				0.19	8.0×10^{14} [e]	4.1%		
NW US Margin, St 2, 4	suboxic	0.3-0.5		0.24				Morford et al. (2005)
NW US Margin, WEC	suboxic	0.3-0.9		0.3				Morford and Emerson (1999); Morford et al. (2005)
Western Canadian Margin	oxic to suboxic	0.4-0.7		0.029				McKay et al. (2007)
Arabian Sea					1.4×10^{16} [j]	71%		
Murray Ridge, PC463	suboxic			0.36				van der Weijden et al. (2006)
ANOXIC								
Cariaco Basin	anoxic			1.34-1.56			1.34	Calvert et al. (2015), new data
Walvis Bay	anoxic		0.11	2.1				Colodner et al. (1993)
Saanich Inlet	seasonally anoxic		0.616	1-1.5				Poirier (2006)
Chile Shelf	anoxic		0.033	3.2				Colodner et al. (1993)
Peru Shelf	intermittently anoxic; upwelling zone		0.0242	0.5				Colodner et al. (1993)
Black Sea	anoxic; restricted		0.0055-0.0078	0.15-0.54				Hay (1988), Hay et al. (1991), Ravizza et al. (1991)

a. Calculated from data of North Atlantic sediments; a value of 1.2×10^{-5} ng $cm^{-2}yr^{-1}$ is chosen. Observed range is 2×10^{-6}–2×10^{-4} ng $cm^{-2}yr^{-1}$
b. Sverdrup et al. (1942)
c. Wollast (2003)
d. Calculated from sedimentation rate and dry bulk density data from Moore et al. (2006) and O'Regan (2007), respectively.
e. Area assumed to be the same as Californian Borderlands
f. Dufour and Ouellet (2007)
g. Davis (1984)
h. Iwanowicz et al. (1973)
i. Reimers et al. (1996)
j. Area affected by denitrification only; Naqvi (1991)

Table 3. Parameters of modern marine Re sink fluxes (see Table 2 for comprehensive literature data used for estimating b_i.)

	% Area Seafloor, k_i	Characteristic Burial Rate, b_i (ng/cm^2/yr)	Sink Flux, F_{out} (mol/yr)	% of Input Flux
Oxic	83.89%	1.60×10^{-3}	2.61×10^{4}	6.08%
Suboxic	4.67%	4.15×10^{-1}	3.75×10^{5}	87.41%
Anoxic	0.11%	1.339	2.80×10^{4}	6.52%

Table 4. Average $[Re]_{sed}$, $[Re]_{sed}$/TOC ratio, and associated standard deviation (1σ) for each stage. To calculate statistical values for each stage, arithmetic mean values were first calculated for each 5 Ma binned interval (time-point means; table S4 in the supplementary database). Stage mean values, bootstrap mean values, and bootstrap 95% confidence intervals were then calculated from these time-point means (see section 4.1). Bootstrap analysis was not performed for stage 2 due to low number of time-binned data (n=2). The anomalous ~1.1 Ga Touirist Formation is excluded from stage 3 calculations.

Stage	Age Interval (Ga)	$[Re]_{sed}$ n*	Mean $[Re]_{sed}$ (ppb)	Bootstrap mean $[Re]_{sed}$ (ppb)	Bootstrap 95% confidence interval	$[Re]_{sed}$ /TOC n*	Mean $[Re]_{sed}$ / TOC (ppb/wt%)	Bootstrap mean $[Re]_{sed}$ / TOC (ppb/wt%)	Bootstrap 95% confidence interval
1	2.72–2.50	9	13	13	10–17	5	5	5	2–7
2	2.50–2.05	2	102	–	–	2	15	–	–
3	2.05–0.61	20	18	25	14–37	9	7	7	5–9
4	0.61–0.00	44	155	151	95–220	35	31	28	18–40

* "n" here denotes the number of time-point means under each stage (table S4 in the supplementary database).

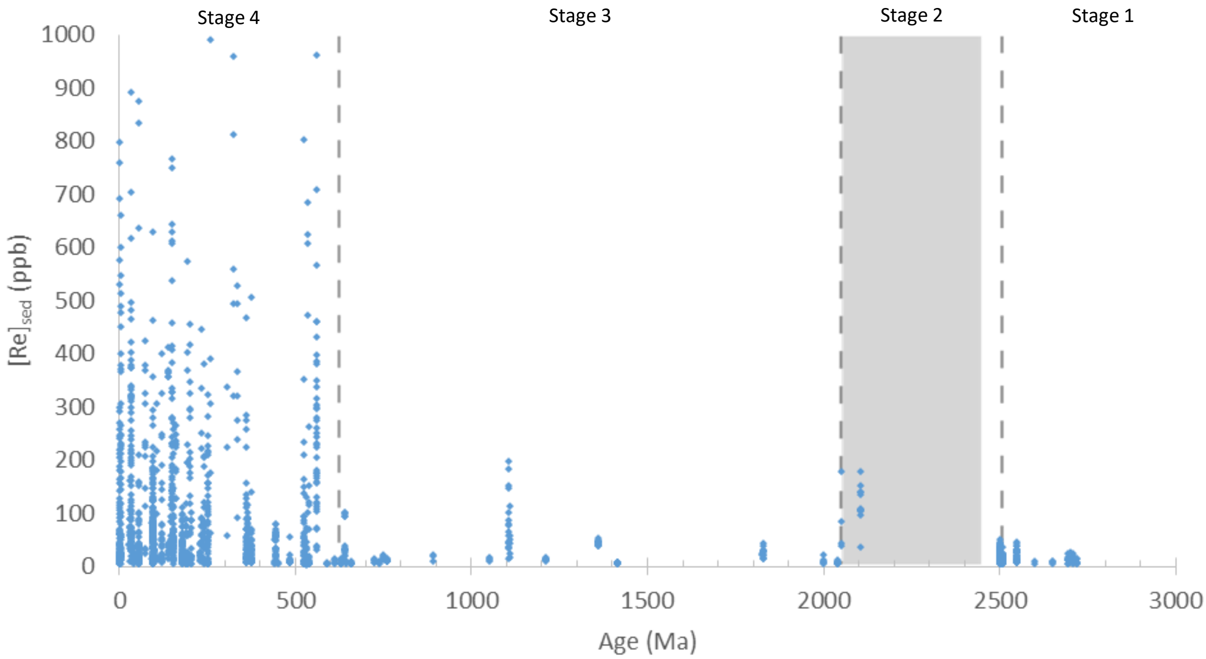

Figure 1. Re concentrations in anoxic, marine organic-rich mudrocks through time (n = 1,768; filtered). Phanerozoic values above 1000 ppb (n = 15) are not displayed. Shaded grey bar represents approximate span of the Great Oxidation Event (GOE).

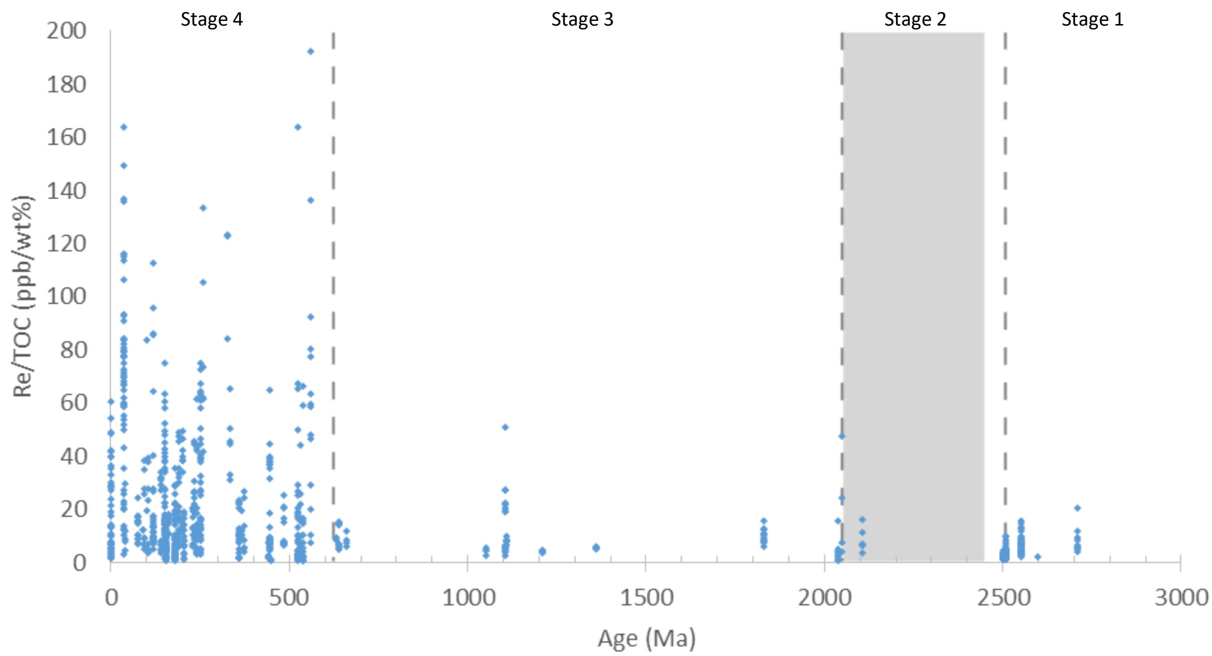

Figure 2. Re concentration normalized to total organic carbon content (TOC) through time (n = 938). Phanerozoic values above 200 ppb/wt% (n = 8) are not displayed.

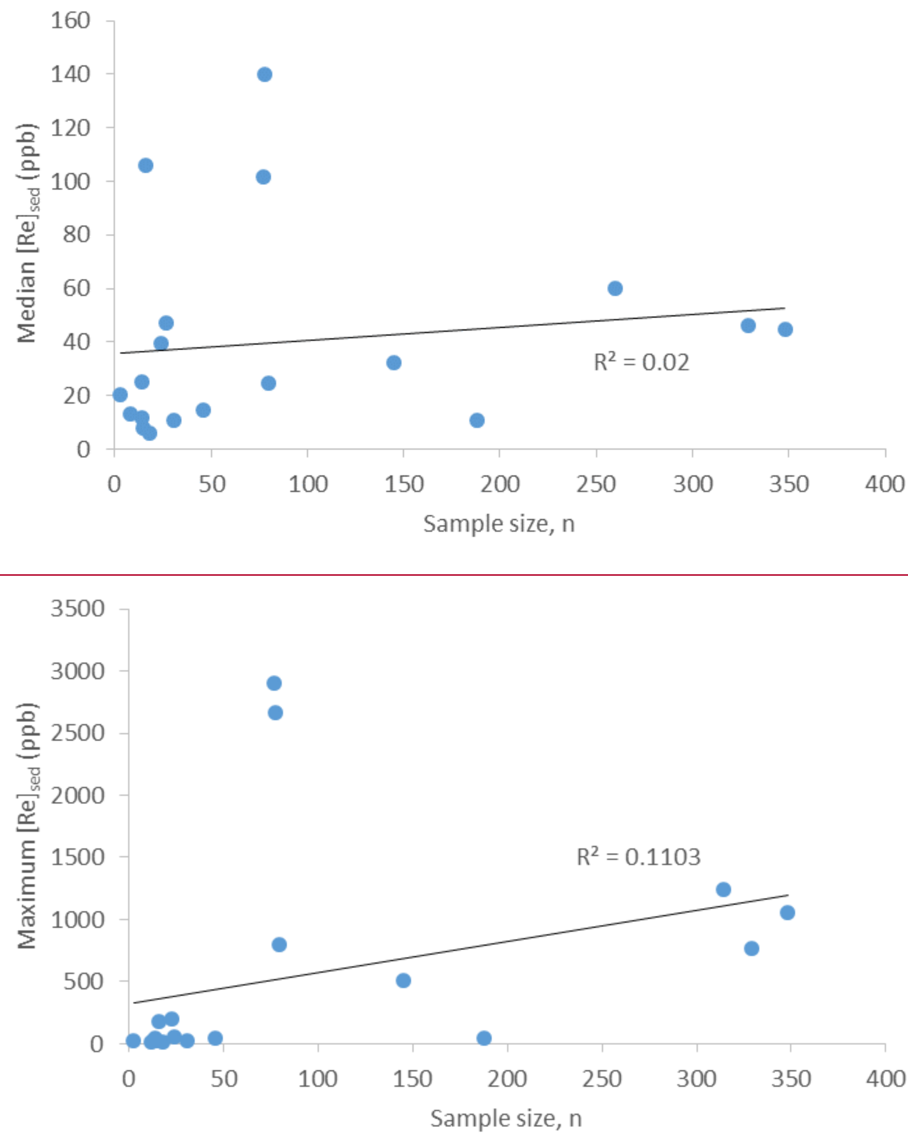

Figure 3. Sample size plotted against ~~maximum~~ median [Re]$_{sed}$ with 100 ~~Ma~~ Myr bins. Sample size and ~~maximum~~ median [Re]$_{sed}$ are not well-correlated (R^2 = 0.02~~1103~~, n = 19, ρ ~~p~~ = 0.~~165~~57).

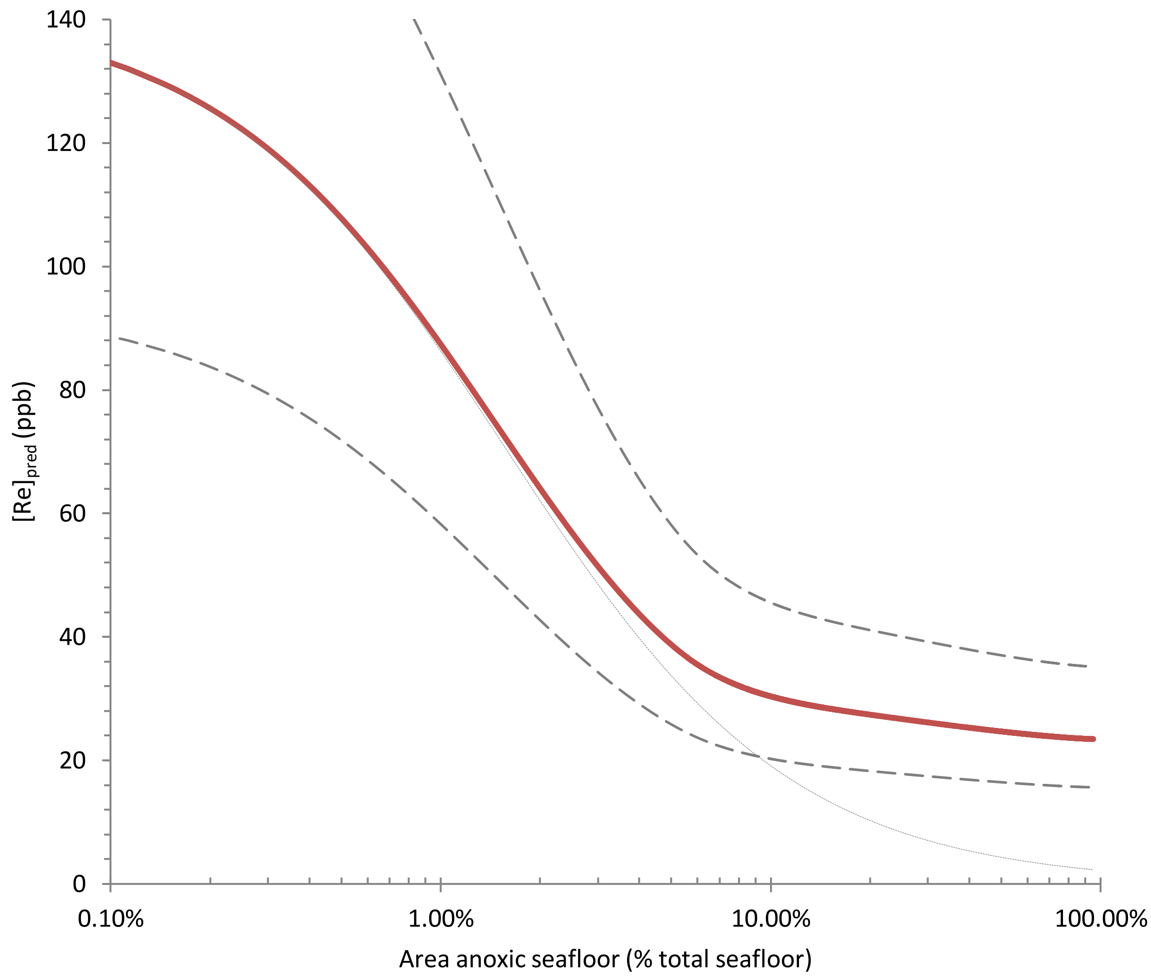

Figure 4. Modeled authigenic Re abundances in anoxic organic-rich mudrocks, $[Re]_{pred}$, versus prescribed extent of anoxia expansion (red curve). Dashed curves represent a factor of 1.5 above and below a bulk mass accumulation rate of 0.01 g $cm^{-2}yr^{-1}$, constrained from the Cariaco Basin. A model assuming a spatially invariant metal burial rate (dotted curve) underestimates the extent of seafloor anoxia for a given $[Re]_{pred}$.

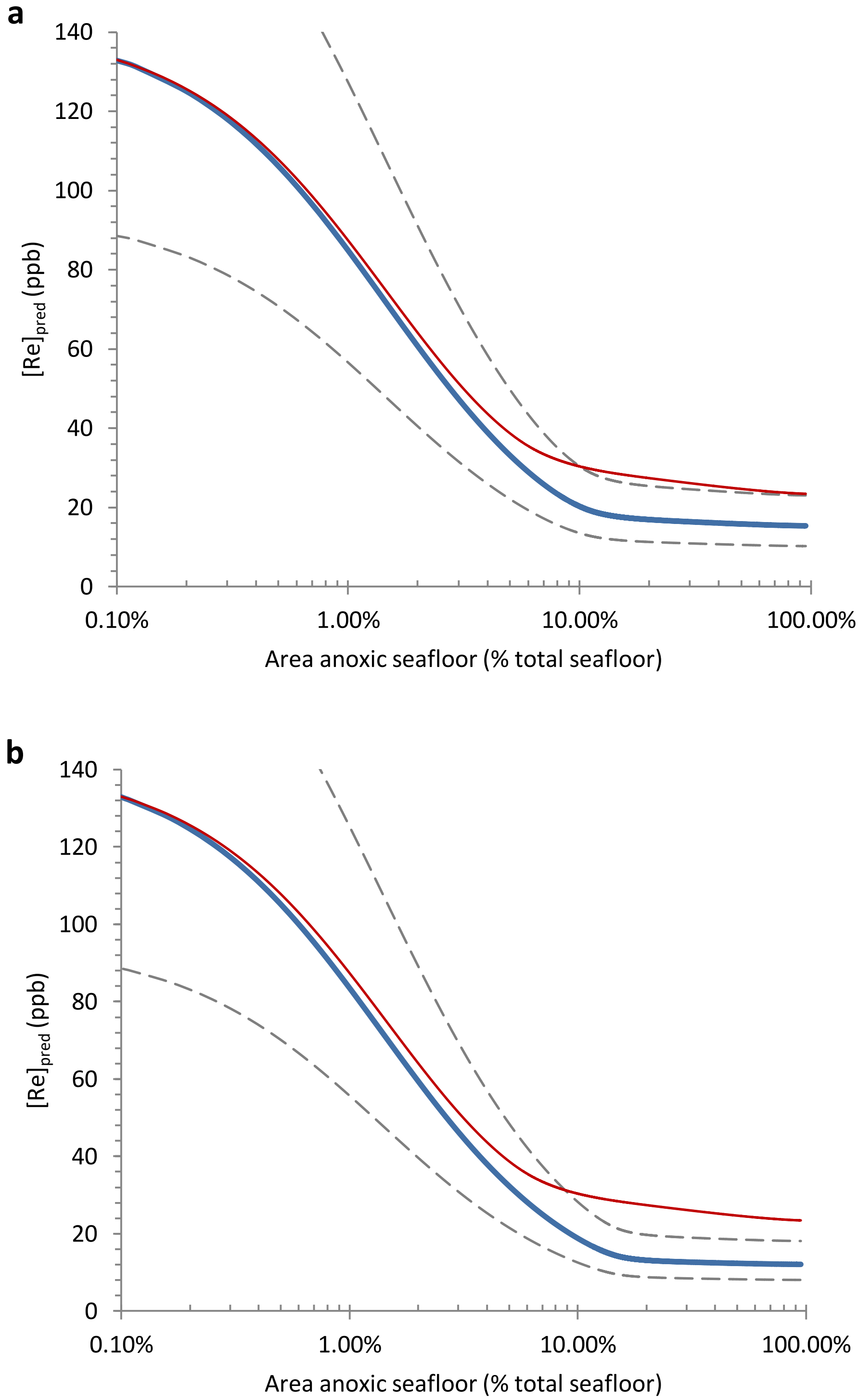

Figure 5. Modeled $[Re]_{pred}$ (blue curve) for an expansion of epeiric seas resulting from a) a 100 m sea level rise, and b) a 200 m sea level rise. Dashed curves represent factor of 1.5 above and below a bulk mass accumulation rate of 0.01 g $cm^{-2}yr^{-1}$. Modeled $[Re]_{pred}$ without epeiric expansion is shown as the red curve for comparison.

Table 5. Mean $[Re]_{sed}$, $[Re]_{sed}$/TOC ratio, and model estimates for the extent of seafloor anoxia of >590 Ma ORM deposited under anoxic bottom water conditions as constrained by $Fe_{HR}/Fe_T > 0.38$ or DOP > 0.45. For each interval, estimates of seafloor anoxia is given for model runs with three different BMAR values (see footnote). Data sources are listed in supplementary data tables.

Stage	Unit Name	Compilation age (Ma)	n	Mean $[Re]_{sed}$ (ppb)	n	Mean $[Re]_{sed}$/TOC (ppb/wt%)	Extent of seafloor anoxia (% seafloor area)		
							Max. BMAR[1]	Mean BMAR[2]	Min. BMAR[3]
1	Carajas Formation	2710	5	12.3	5	7.6	100%	100%	100%
	Upper Nauga Formation	2550	4	22.3	4	6.6	7%	100%	100%
	Klein Naute Formation	2510	30	13.5	30	3.0	100%	100%	100%
	Mt.McRae Shale	2500	28	25.1	24	2.4	5%	43%	100%
2	Sengoma Argillite Formation	2105	6	114.4	6	8.6	0%	0%	1%
	Zaonezhskaya Formation	2050	1	85.3	1	47.4	0%	1%	3%
3	Rove Formation, Canada	1825	11	26.6	11	10.2	5%	26%	100%
	Lower Velkerri Formation	1415	1	5.8			100%	100%	100%
	Upper Velkerri Formation	1360	6	44.2	6	5.7	2%	4%	13%
	Arctic Bay, Victoria Bay, Athole Point Formations	1050	2	13.9	2	3.8	100%	100%	100%
	Black River Dolomite	640	10	65.0	10	10.4	1%	2%	4%

[1] Maximum BMAR = 0.01 g cm^{-2} yr^{-1} × 1.5

[2] Mean BMAR = 0.01 g cm^{-2} yr^{-1}

[3] Minimum BMAR = 0.01 g cm^{-2} yr^{-1} / 1.5